# Natural and artificial fractures response characterisation in large-size samples using distributed acoustic sensing technology

Martuganova, E.M.; Buisman, M.; Barnhoorn, A.

**DOI**
10.3997/2214-4609.2023101461

**Publication date**
2023

**Document Version**
Final published version

**Citation (APA)**
Martuganova, E. M., Buisman, M., & Barnhoorn, A. (2023). *Natural and artificial fractures response characterisation in large-size samples using distributed acoustic sensing technology*. Paper presented at 84th EAGE ANNUAL Conference and Exhibition 2023, Vienna, Austria. https://doi.org/10.3997/2214-4609.2023101461

# Natural and artificial fractures response characterisation in large-size samples using distributed acoustic sensing technology.

E. Martuganova[1], M. Buisman[1,2], A. Barnhoorn[1]

[1] TU Delft; [2] Port of Rotterdam

## Summary

We conducted laboratory experiments using large-scale samples (height: 0.47, diameter: 0.39 m) of basalt and marble coiled with telecommunication fibre. The fibre optical cable was converted to an array of densely spaced receivers (0.01 m) using distributed acoustic sensing (DAS) technology, and the source was placed on top of the samples. We demonstrate with an active acoustic setup how we can capture both the natural and artificial fracture responses. Therefore, this work investigates the applicability of the DAS method for seismic imaging on the lab scale for further technological advancement of vertical seismic profiling using DAS.

## Introduction

Developing carbon capture storage (CCS) and geothermal reservoirs require a comprehensive understanding of geological structures and stress conditions. The characterisation of the faults and fractures plays a vital role in the assessment of the uncertainties and risks related to subsurface operations. Although seismic methods allow imaging of fractured reservoirs with high resolution at significant depths (Casini et al., 2010; Hloušek et al., 2015; Lim et al., 2020; Salaun et al., 2020; Martuganova et al., 2022), understanding the fracture characteristics using active seismic methods and detailed assessment of induced strain and its association with recorded seismic signals still remains challenging.

Monitoring using distributed acoustic sensing (DAS) technology allows cost-effective and nearly continuous data recording using fibre optical cables, which create a receiver array with a dense spacing. Time-lapse DAS vertical seismic profiling has proven to be a reliable technique for monitoring CO2 storage facilities (Correa et al., 2019; Götz et al., 2018; Wilson et al., 2021). In this work we investigate the applicability of DAS for high resolution fracture imagining on a laboratory scale. Moreover, our experimental work aims to improve the quantification of the fault/fracture responses using fibre optical data. An accurate estimation of the fracture response allows us to better understand and estimate the effects of fractures in the reservoir areas and improve seismic monitoring method.

## Experiment setup

We used large marble and basalt and marble blocks for our experiments which were collected from the outcrop around Kızıldere geothermal site in Turkey (Janssen et al., 2021) and the Hellisheiði geothermal field in Iceland (Janssen et al., 2022), respectively. We will refer to the marble sample as Kevin and the basalt as Bob (see Figure 1a). The height of both samples is the same, namely 0.474 m; the diameter equals 0.388 m (Figure 1b). The marble Kevin has a natural fracture occurring at around 0.056 m from the top of the sample. To simulate a similar fracture in basalt Bob, the top part of the sample was sawed through to create an artificial fracture. Thus, these two samples serve as a good approximation for homogeneous low porosity (Kevin, Figure 1c), and highly porous and heterogeneous (Bob, Figure 1d) reservoirs. As a source, we used The Simrad 38/200 Combi D transducer, of which we only used the transducer with a centre frequency of 38 kHz to emit a pulse with a 16 kHz central frequency. The output of the wave generator was plugged into the amplifier, which was connected to the transducer. The resulting source signal in the time domain is shown in Figure 1e. The frequency spectrum has a peak at 16kHz (Figure 1f) but is distorted by the amplifier and thus shows a range of frequencies between 8 at 30kHz and artefact signals at around 6kHz. As a receiver, a standard telecommunication fibre with a diameter of 0.0016 m was tightly coiled around both samples and connected to the interrogator unit from Alcatel Submarine Networks (ASN) (Waagaard et al., 2021). This allowed us to create a vertical seismic profiling (VSP) setup with a dense array of receivers with 0.01 m spacing in sample's height. We set the gauge length for the marble Kevin to 15 m and the basalt Bob to 25 m. The gauge length was selected by finding a compromise between good signal penetration through the whole sample and the finest resolution possible.

## Results

Figure 2 shows two seismic sections for the marble and basalt samples. The processing of the data included stacking the individually recorded source signal bursts sent by the wave generator, each 5 or 10 ms, to improve signal-to-noise ratio. Strain data recorded using marble Kevin has a very distinct first arrival (blue arrow, Figure 2a) and complex interference of the reflections (see violet arrow, Figure 2a) and multiples. Most interestingly, a fracture zone is clearly visible. Firstly, at the sample length corresponding to the fracture, we can see multiple phase discontinuities and amplitude variations (for instance, the green arrow in Figure 2a). Furthermore, at around 0.6 ms there is a V-shaped structure (magenta arrow, Figure 2a), which could potentially correspond to the reflection from the fracture. The time difference between the sample's top and bottom equals 0.0084 ms. Considering the sample's height, this gives a 5642.86 m/s velocity estimation for the whole sample, which agrees with the P-wave estimation interval 5500-5800 m/s from Janssen et al. (2021). Basalt Bob has a distinct difference in the appearance

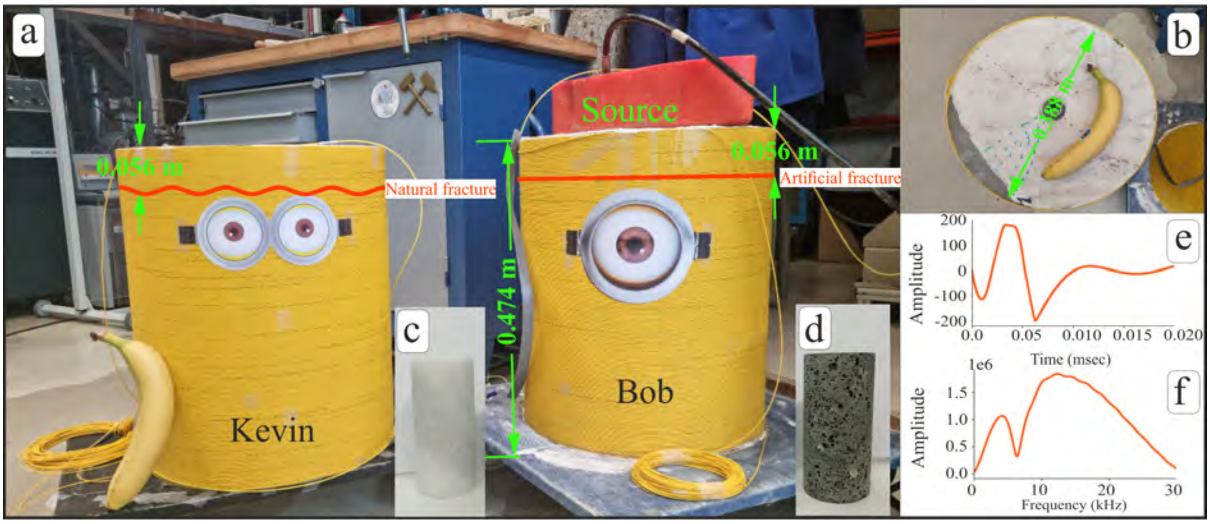


***Figure 1*** *(a) The laboratory setup showing the marble and basalt samples coiled in fibre and the Simrad 38/200 Combi D transducer location. Wavy orange and solid lines show known locations of the natural and artificially created fractures in the marble Kevin and basalt Bob, respectively. (b) A top view of the Marble sample. Photos of similar smaller cores for marble (c) and basalt (d) rocks. (e) The source signal function in the time domain after amplification. (f) Frequency spectrum of the source with a central frequency at 16 kHz.*

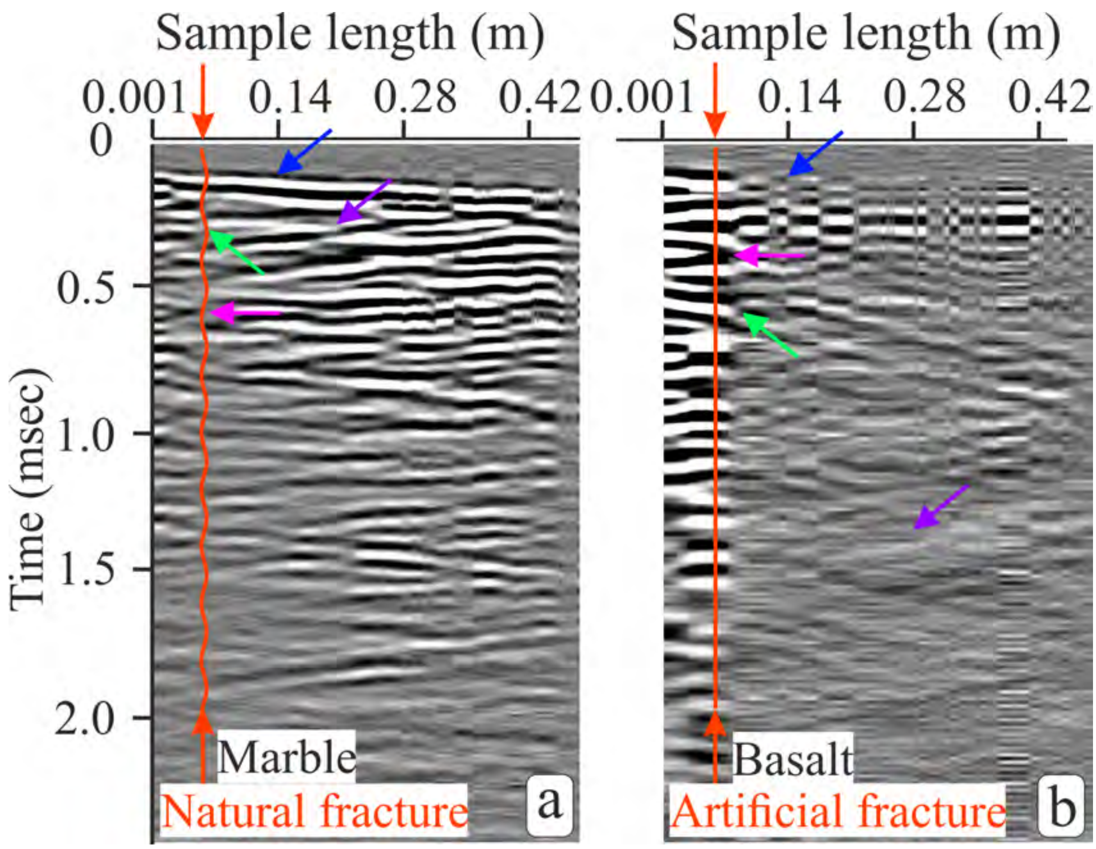


***Figure 2*** *Seismic sections for the (a) marble and (b) basalt samples. Colored arrows (exemplary): direct downgoing P-wave (dark blue), V-shaped reflections from the top of the fracture (magenta), reflections in the lower part of the samples (violet), phase discontinuities (light green). Wavy orange and solid lines show known locations of the natural and artificially created fractures in the marble Kevin and basalt Bob, respectively.*

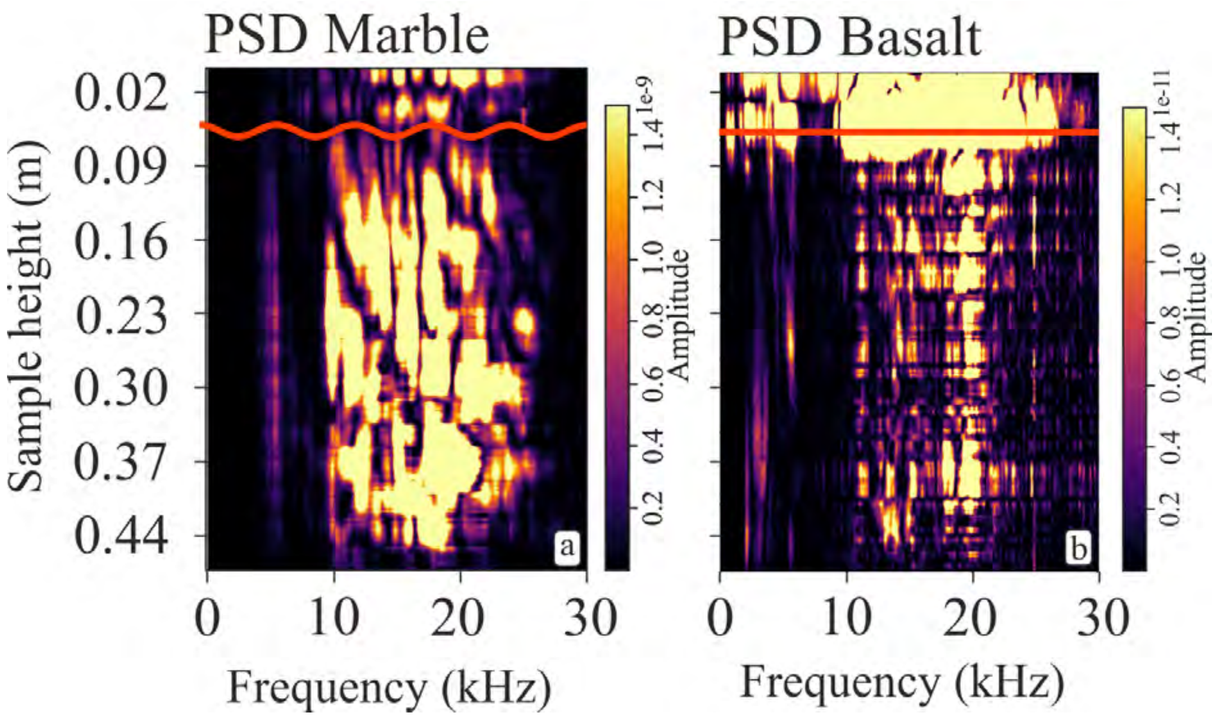


***Figure 3*** *Power spectral density calculated for marble Kevin and basalt Bob. Wavy orange and solid lines show known locations of the natural and artificially created fractures in the marble Kevin and basalt Bob, respectively.*

of the seismic data in the time domain. We can mainly see numerous reverberations in the top part of the sample that look like high-amplitude stripy reflections. The amount of energy which travels down passing the fracture area is significantly lower than for the marble sample. The first arrival (blue arrow, Figure2b) is very poorly visible, as well as reflections and multiples. Although the signal-to-noise ratio is very poor for the lower part of the basalt, curiously enough, we still can see some low frequent reflections (violet arrow, Figure 2b).

In the frequency domain (Figure 3), the difference in sample fracture responses becomes even more apparent. The upper part of the marble Kevin power spectral density (PSD) plot (Figure 3a), before the fracture, shows repetitive maxima. Then there is a discontinuation in amplitude, corresponding to the natural fracture response. The lower part of the marble sample PSD has elongated, irregularly shaped high amplitude areas in the frequency range between 10 to 28 kHz, which roughly coincides with the source frequencies range. A line at around 6 kHz corresponds to the artefact occurring due to the distortion by the amplification. Basalt Bob's PSD (Figure 3b) shows mainly energy accumulated in reverberations in the upper part of the sample before the artificial fracture. The lower part of the sample on the PSD has significantly lower amplitudes; the main energy is focused at around 20kHz. Some smaller high amplitude zones are noticeable between 10 and 28kHz, which vary with the sample height. The fracture zone area is shown beyond the exact location due to more averaging by the larger gauge length, which causes, the smearing of the amplitude.

**Conclusions and Outlook**

With our laboratory work, we created a VSP setup by using thinly coiling an optical fibre around a basalt and marble cylinders. Each seismogram allows the connection of the depth information (sample) height with the time domain directly to characterise the structure of reservoir rock samples. With this simple active acoustics setup, we show that we can capture both artificial and natural fractures in potential reservoir outcrops. Further tests for the cable coupling improvement tests for the basalt Bob are planned, including applying the rubber sleeve and a coupling agent. After improving the signal-to-noise ratio, we plan to conduct measurements at elevated stress conditions to study the signature of fractures on seismic wave propagation in more detail, develop a workflow for the lab vertical seismic profiling, which includes the application of the smooth inversion method (Lizarralde and Swift, 1999) to calculate the velocity profile for the whole sample to acquire a 3D seismic image of the sample. The resulting seismic image can be compared with similar smaller CT scan images of the analogous reservoir samples. Further lab work includes studying and quantifying the strain applied for fracture opening with the recorded seismic signals using distributed acoustic sensing technology.

**Acknowledgements**

We would like to thank Jens van den Berg, Mark Friebel and Karel Heller for providing technical support for organising the experimental work and Prof. Dr. Karl-Heinz Wolf for arranging access to the samples. Additionally, the authors would like to acknowledge Barbara Perez Salgado for helping wrap the samples with fibre and creating Bob and Kevin. This contribution is part of the SHARP Storage research program (‘Stress History and reservoir pressure for improved quantification of CO2 storage containment risks’) funded through ACT3– Accelerating CCS Technologies (Project No ACT320011).

**References**

Casini, M., Ciuffi, S., Fiordelisi, A., Mazzotti, A. and Stucchi, E. [2010] Results of a 3D seismic survey at the Travale (Italy) test site. *Geothermics*, **39**(1), 4–12.

Correa, J. [2018] *Distributed Acoustic Sensing for Seismic Imaging and Reservoir Monitoring Applied to CO2 Geosequestration*. Ph.D. thesis, Curtin University. (last access: 1 April 2022).

Correa, J., Pevzner, R., Bona, A., Tertyshnikov, K., Freifeld, B., Robertson, M. and Daley, T. [2019] 3D vertical seismic profile acquired with distributed acoustic sensing on tubing installation: A case study from the CO2CRC Otway Project. *Interpretation*, **7**(1), SA11–SA19.

Götz, J., Lüth, S., Henninges, J. and Reinsch, T. [2018] Vertical seismic profiling using a daisy-chained deployment of fibre-optic cables in four wells simultaneously – Case study at the Ketzin carbon dioxide storage site. *Geophysical Prospecting*, **66**(6), 1201–1214.

Hloušek, F., Hellwig, O. and Buske, S. [2015] Three-dimensional focused seismic imaging for geothermal exploration in crystalline rock near Schneeberg, Germany. *Geophysical Prospecting*, **63**(4), 999–1014.

Janssen, M., Draganov, D., Bos, J., Farina, B., Barnhoorn, A., Poletto, F., Otten, G.V., Wolf, K. and Durucan, S. [2022] Monitoring Co2 Injection into Basaltic Reservoir Formations at the Hellisheiði Geothermal Site in Iceland: Laboratory Experiments. In: *Conference Proceedings, the 83rd EAGE Annual Conference and Exhibition*, Madrid, Spain, 6-9 June 2022. 1–5.

Janssen, M.T.G., Barnhoorn, A., Draganov, D., Wolf, K.H.A.A. and Durucan, S. [2021] Seismic Velocity Characterisation of Geothermal Reservoir Rocks for CO2 Storage Performance Assessment. *Applied Sciences*, **11**(8).

Lim, T., Fujimoto, A., Kobayashi, T. and Mondanos, M. [2020] DAS 3DVSP Data Acquisition for Methane Hydrate Research. In: *Conference Proceedings, EAGE Workshop on Fiber Optic Sensing for Energy Applications in Asia Pacific*, Kuala Lumpur, Malaysia, 9-11 November 2020. 1–5.

Lizarralde, D. and Swift, S. [1999] Smooth inversion of VSP traveltime data. *Geophysics*, **64**(3), 659–661.

Martuganova, E., Stiller, M., Norden, B., Henninges, J. and Krawczyk, C.M. [2022] 3D deep geothermal reservoir imaging with wireline distributed acoustic sensing in two boreholes. *Solid Earth*, **13**(8), 1291–1307.

Salaun, N., Toubiana, H., Mitschler, J.B., Gigou, G., Carriere, X., Maurer, V. and Richard, A. [2020] High-resolution 3D seismic imaging and refined velocity model building improve the image of a deep geothermal reservoir in the Upper Rhine Graben. *The Leading Edge*, **39**(12), 857–863.

Waagaard, O.H., Rønnekleiv, E., Haukanes, A., Stabo-Eeg, F., Thingbø, D., Forbord, S., Aasen, S.E. and Brenne, J.K. [2021] Real-time low noise distributed acoustic sensing in 171 km low loss fiber. *OSA Continuum*, **4**(2), 688–701.

Wilson, G.A., Willis, M.E. and Ellmauthaler, A. [2021] Evaluating 3D and 4D DAS VSP image quality of subsea carbon storage. *The Leading Edge*, **40**(4), 261–266.